MedChemComm

RESEARCH ARTICLE

View Article Online
View Journal | View Issue

Cite this: *Med. Chem. Commun.*, 2019, **10**, 2111

Preparation and clinical translation of ^{99m}Tc-PSMA-11 for SPECT imaging of prostate cancer

Kusum Vats,[a] Kanhaiyalal Agrawal,[c] Rohit Sharma,[ad] Haladhar Dev Sarma,[b] Drishty Satpati *[ad] and Ashutosh Dash[ad]

Received 19th August 2019,
Accepted 15th October 2019

DOI: 10.1039/c9md00401g

rsc.li/medchemcomm

This study explores the feasibility of radiolabeling the HBED-CC-PSMA (PSMA-11) ligand with Tc-99m for SPECT imaging of prostate cancer patients. ^{68}Ga-HBED-CC-PSMA (PSMA-11) is used clinically for PET/CT imaging of prostate cancer (PCa) patients. However, a PET/CT facility may not be affordable and/or accessible to remotely located health centers. Thus, economic considerations require development of a SPECT-based tracer to provide low cost effective health care to the entire global population. Hence, radiochemical parameters were varied and optimized to obtain the maximum radiochemical yield of ^{99m}Tc-PSMA-11. ^{99m}Tc-PSMA-11 could be prepared in 60 ± 5% radiochemical yield and >98% radiochemical purity with a specific activity of 15 ± 5 GBq μmol^{-1}. The radiotracer exhibited high stability *in vitro* in human serum after 24 h. A cell uptake of 15.2 ± 1.2% was observed for ^{99m}Tc-PSMA-11 in PSMA-positive prostate carcinoma LNCaP cells. Rapid clearance from blood, liver, intestine, lungs and other major organs was observed during normal biodistribution studies. The radiotracer, ^{99m}Tc-PSMA-11, exhibited physiological distribution in salivary and lacrimal glands similar to that of ^{68}Ga-PSMA-11 in mice and successfully identified primary tumors as well as metastatic lesions in human patients. This study thus highlights successful radiolabeling of HBED-CC-PSMA with Tc-99m and the potential of ^{99m}Tc-PSMA-11 as a SPECT imaging agent for PCa.

Introduction

In the molecular prostate cancer imaging arena, nuclear medicine has rapidly evolved for accurate assessment of the disease through development of radiotracers, thus playing key role in primary diagnosis, staging and re-staging of cancer, and monitoring of patients for treatment response and biochemical relapse.[1–3] Early prostate cancer detection would aid in guiding therapeutic decisions and precise targeted treatment for improved patient care.[2,3] Dedicated research and investigations have led to development of several prostate cancer imaging PET tracers that have entered the clinical domain which include ^{18}F-choline, ^{11}C-choline, ^{18}F-fluciclovine (anti-1-amino-3-^{18}F-fluorocyclobutane-1-carboxylic acid; FACBC), ^{68}Ga-PSMA-11, ^{18}F-PSMA-1007, ^{18}F-DCFBC and ^{18}F-DCFPyl.[4–11] Amongst them, ^{68}Ga-PSMA-11 targeting prostate specific membrane antigen (PSMA) over-expression has made a remarkable clinical impact globally on prostate cancer management.[12–15] ^{68}Ga-PSMA PET exhibits excellent diagnostic performance for detection of primary and metastatic prostate cancer.[16–18] PET/CT is a valuable imaging tool offering advantages of possible quantification and high resolution images but is constrained by higher financial investment, availability of ^{68}Ge/^{68}Ga generators and/or proximity to a cyclotron.[19,20] Development of a corresponding single photon emission computed tomography (SPECT) tracer however would further expedite the detection and assessment of prostate cancer patients as a SPECT/CT imaging facility would require lower financial investment and can be easily expanded to remote and distant locations.[21] Although SPECT/CT suffers from a few drawbacks, it still accounts for the maximum number of scans worldwide due to economic factors and easy availability of long-lived gamma-emitting isotopes.[20] The enormous use of SPECT radioisotope technetium-99m for diagnostic scans is attributed to its nuclear decay characteristics ($t_{1/2}$ = 6 h, E_γ = 140 keV), worldwide availability of ^{99}Mo/^{99m}Tc generators and simple preparation of ^{99m}Tc-radiopharmaceuticals using ready-to-use kits at hospital radiopharmacy.[22,23] Various advances in instrumentation and software have now enabled quantification of SPECT/CT images.[24] Hence in the pursuit of development of a SPECT-based PSMA radioligand, various

[a] *Radiopharmaceuticals Division, India. E-mail: drishtys@barc.gov.in; Fax: +91 22 25505151; Tel: +91 22 25590748*
[b] *Radiation Biology and Health Science Division, Bhabha Atomic Research Centre, Mumbai-400085, India*
[c] *Department of Nuclear Medicine, All India Institute of Medical Sciences, Bhubaneswar-751019, India*
[d] *Homi Bhabha National Institute, Anushaktinagar, Mumbai-400094, India*

^{99m}Tc-labeled agents are being currently investigated.[25–29] The PSMA targeting ligands developed are mainly small molecules based on the pharmacophore Glu-urea-Lys which binds with the active site of the PSMA enzyme and acts as its inhibitor. To facilitate ^{99m}Tc-labeling, this binding motif has been conjugated with chelators like mercaptoacetyl triserine (MAS3),[27,29] carboxylic acid-substituted imidazoles[25,26] and hydrazinonicotinic acid (HYNIC)[28] to prepare radiotracers ^{99m}Tc-PSMA-I&S, ^{99m}Tc-MIP-1404 and ^{99m}Tc-HYNIC-PSMA, respectively. Preliminary patient imaging studies have been reported for these radiotracers utilizing ^{99m}Tc-HYNIC, $(^{99m}TcO)^{3+}$ and $[^{99m}Tc(CO)_3]^+$ cores.[26,29,30]

Conjugation of different chelators with the biological targeting ligand may result in altered pharmacokinetics due to the altered charge, lipophilicity and targeting ability.[31,32] Since ^{68}Ga-PSMA-11 has displayed favorable clinical results, we were interested in investigating the feasibility of using the same ligand for preparation of a ^{99m}Tc-labeled tracer.[13–15] The PSMA-11 ligand constitutes the acyclic chelator HBED-CC (*N*,*N*′-bis-[2-hydroxy-5-(carboxyethyl)benzyl]ethylenediamine-*N*,*N*′-diacetic acid) which has been used for Ga-68 chelation. The chelator HBED-CC contains carboxylic acid groups, nitrogen atoms and hydroxyl groups which are capable of coordinating and forming a stable complex with Tc-99m.[33,34] Therefore, in this work we have explored the possibility of Tc-99m labeling of an HBED-CC conjugated PSMA targeting ligand, PSMA-11. Towards this, experiments were performed to optimize the radiolabeling parameters and quality control procedures. Stability studies of ^{99m}Tc-PSMA-11, *in vitro* cellular uptake measurements and *in vivo* pharmacokinetic pattern determination were carried out. Preliminary clinical evaluation of the SPECT radiotracer was also performed in prostate cancer patients.

Materials and methods

Reagents and instruments

Solvents and chemicals were purchased from Aldrich (Milwaukee, WI) unless stated otherwise and used without further purification. The ligand PSMA-11 was purchased from ABX advanced biochemical compounds (Biomedizinische Forschungsreagenzien GmbH, Radeberg, Germany). Stannous chloride dihydrate was procured from Fluka. Human prostate carcinoma LNCaP and PC3 cells were obtained from the National Center for Cell Sciences (NCCS) Pune, India. High-performance liquid chromatography (HPLC) grade water was obtained from Merck. All other solvents and chemicals were purchased from Sigma Aldrich, USA. All radioactive counting associated with the radiochemical studies was carried out using a well-type NaI(Tl) scintillation gamma counter (Electronic Corporation of India Limited, India). The analytical HPLC measurements were performed on a JASCO PU 2080 Plus dual pump HPLC system, Japan, with a JASCO 2075 Plus tunable absorption detector and a Gina Star radiometric detector system, using a C18 reversed phase HiQ Sil column (5 μm, 4 × 250 mm). The eluting solvents (1 mL min^{-1}) used in HPLC were: H_2O (solvent A) and acetonitrile (solvent B) with 0.1% trifluoroacetic acid following the gradient: 0–28 min: 90% A–10% A; 28–30 min: 10% A; 30–32 min: 10% A–90% A.

Radiochemistry

Radiolabeling parameters like the amount of ligand, reducing agent and pH of the reaction mixture were optimized to obtain the maximum radiochemical yield (Table 1). The ligand amount was varied between 10 and 70 μg and that of $SnCl_2$ from 20–80 μg. Radiolabeling was carried out at different pH values (3, 5 and 7) to study the effect on the radiochemical yield. ^{99m}Tc-labeling of the PSMA-11 ligand was then performed under optimized conditions. The ligand (50 μg, 53 nmol) was dissolved in distilled water and $Na^{99m}TcO_4$ (500 μL, 740 MBq) and $SnCl_2$ (40 μg) were added to this solution. The pH of the final reaction mixture was 5.0–5.5. The reaction mixture was heated at 90 °C for 15 min and subsequently cooled for performing radiochemical yield (RCY) and purity (RCP) analyses by TLC and HPLC. TLC analysis was carried out using two different mobile phases. The formation of ^{99m}Tc-colloid was determined using water/acetonitrile (1 : 1) as the solvent, whereas the extent of $^{99m}TcO_4^-$ was estimated with methyl ethyl ketone (MEK) as the mobile phase.

The radiolabeled preparation was passed through a 0.22 μm sterile filter before performing any *in vitro* or *in vivo* animal studies/patient studies.

The partition coefficient for ^{99m}Tc-PSMA-11 was measured between *n*-octanol and water. The radiotracer (50 μL, ~3.7 MBq) was mixed with distilled water (950 μL) and *n*-octanol (1 mL) and shaken vigorously for 1 min followed by centrifugation (3500*g*) for 5 min to get clear separation of the two layers. The radioactivity in equal aliquots of the two layers (100 μL) was measured in a gamma-counter. The experiment was repeated thrice to calculate the $\log P_{o/w}$ of the radiotracer.

The patient dose of ^{99m}Tc-PSMA-11 was formulated by addition of $^{99m}TcO_4^-$ (1.48 GBq) and $SnCl_2$ (40 μg) to the ligand (50 μg). Incubation at 90 °C for 15 min was followed by filtration through a 0.22 μm syringe filter.

Table 1 Optimized radiolabeling parameters and quality control of ^{99m}Tc-PSMA-11

Radiolabeling parameters	
Precursor amount	50 μg
Stannous chloride	40 μg
pH	5
Heating	90 °C, 15 min
Quality control	
Radiochemical yield (TLC)	60 ± 5% (n = 10)
Radiochemical purity (HPLC)	
Sep pak purification	92 ± 1%
Filtration	98 ± 1%

In vitro studies

***In vitro* stability.** The *in vitro* stability was evaluated by incubation of ^{99m}Tc-PSMA-11 in saline at room temperature for 6 h. Human serum for serum stability studies was obtained from healthy volunteers at Bhabha Atomic Research Center Hospital. Serum stability was determined by incubating the radiolabeled solution (0.1 mL) with human serum (0.9 mL) for 6 h at 37 °C. Aliquots were withdrawn at 1, 6 and 24 h and upon precipitation of proteins with acetonitrile samples were injected in the HPLC. The stability of the radiotracer was estimated by the change in the peak profile and retention time in the HPLC radiochromatogram.

Cell uptake studies. Prostate carcinoma cells, LNCaP (PSMA-positive) and PC3 (PSMA-negative), were cultured in Dulbecco's modified Eagle's medium (DMEM) supplemented with 10% fetal calf serum (Invitrogen Carlsbad, CA) and 1% antibiotic/antimycotic formulation and incubated at 37 °C in a humidified atmosphere containing 5% CO_2. The cells (1×10^5) were seeded in 24-well tissue culture plates and incubated at 37 °C overnight. Subsequently, the cells were incubated with ^{99m}Tc-PSMA-11 (8 pmol, 37 kBq per well), at 37 °C for 1 h. After 1 h, the cells were washed with ice-cold phosphate buffer saline, solubilized with 1.0 M NaOH (1 mL) and measured for radioactivity using a NaI (Tl) gamma counter. Inhibition studies were performed under similar experimental conditions wherein a 100-fold excess of PSMA-11 was used for blocking receptors.

In vivo studies

In vivo biodistribution studies were carried out on normal Swiss mice at 3 h p.i. (n = 4). The radiotracer (~3.7 MBq per animal, 12 pmol, 100 μL) was injected intravenously into the tail vein of each mouse (n = 4). The animals were sacrificed, the relevant organs were excised and weighed, and the activity associated with them was measured in a flat-bed type NaI(Tl) counter with a suitable energy window for Tc-99m. The activity retained in each organ/tissue was expressed as a percent value of the injected dose per gram (% ID g^{-1}). All animal procedures were performed in accordance with the Guidelines for Care and Use of Laboratory Animals approved by the Social Justice and Empowerment Committee for the Purpose of Control and Supervision of Experiments on Animals (CPCSEA), Government of India. The experimental protocols were approved by the Bhabha Atomic Research Center Animal Ethics Committee (BAEC).

Clinical studies

In the preliminary study, a ^{99m}Tc-PSMA-11 scan was performed in two patients with suspected prostate carcinoma. All experiments were performed in accordance with the "National ethical guidelines for biomedical and health research involving human participants, Indian Council of Medical Research 2017", and the experiments were approved by the ethics committee at All India Institute of Medical Sciences, Bhubaneswar, India. Written informed consent was obtained from human participants before administration of the radiotracer. Whole body SPECT/CT imaging (Tandem Discovery 670, GE Healthcare) was performed after intravenous administration of 259–370 MBq ^{99m}Tc-PSMA-11. Furosemide injection was administered 30 minutes after administration of the radiopharmaceutical. Whole body and spot view of pelvis images were acquired at 1 h and 3 h after radiopharmaceutical injection. SPECT–CT images of the pelvis and any other region with abnormal uptake were acquired.

Results and discussion

Radiochemistry

A standard 'wet chemistry' protocol was followed for Tc-99m labeling of PSMA-11 (Fig. 1). The ligand amount required to achieve the maximum radiochemical yield was optimized by performing radiolabeling with various quantities of PSMA-11 (10, 20, 40, 50 and 70 μg) (Fig. 2A). During preparation of ^{99m}Tc-PSMA-11, it was observed that free $^{99m}TcO_4^-$ and colloidal Tc-99m decreased on increasing the ligand amount. The best radiochemical yield of 60 ± 5% was obtained with 50 μg of ligand which did not increase any further on increasing the PSMA-11 amount. The remaining activity (30–35%) was present in colloidal form that could not be reduced by increasing the ligand quantity. In an attempt to reduce the ^{99m}Tc-colloid, radiolabeling was performed by changing the $SnCl_2$ content (20–80 μg) but it did not give any positive results (Fig. 2B). The radiochemical yield remained the same

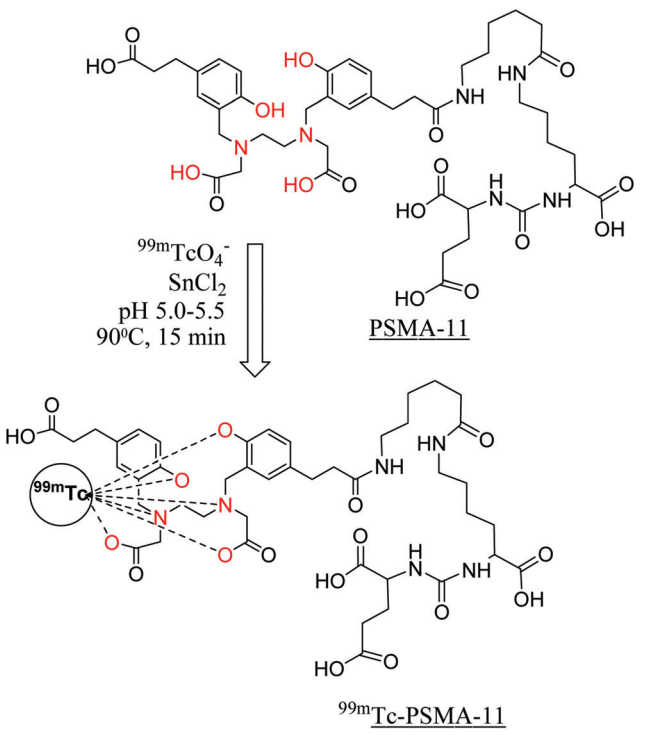

Fig. 1 Schematic presentation of radiochemical formulation of PSMA-11 indicating possible coordination sites (in red) and probable ^{99m}Tc-complexation.

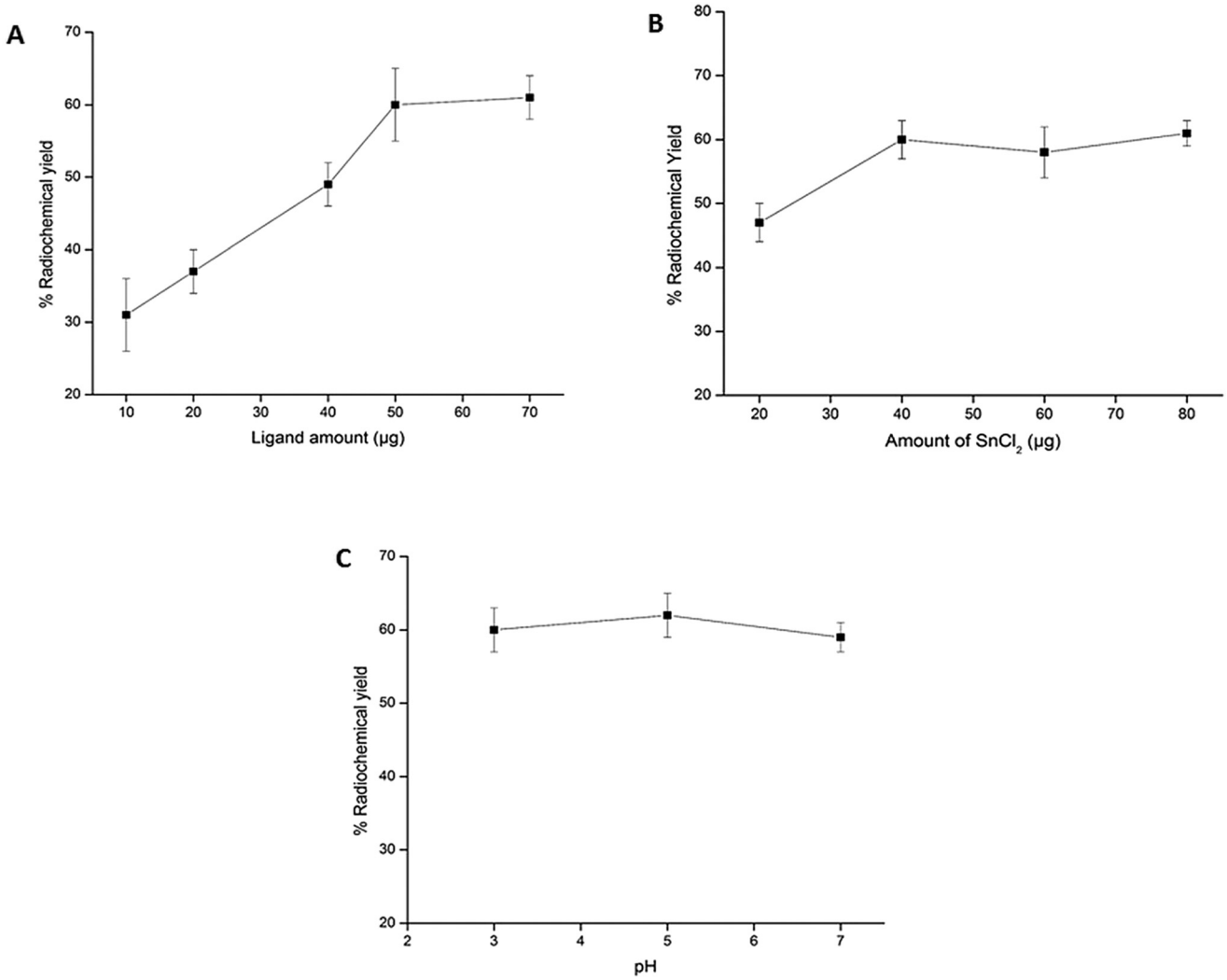

Fig. 2 Optimization of the (A) ligand amount, (B) amount of $SnCl_2$ and (C) pH to obtain the maximum radiochemical yield of ^{99m}Tc-PSMA-11.

irrespective of the pH of the reaction mixture (3, 5 or 7) (Fig. 2C). Optimized radiolabeling conditions are presented in Table 1.

The HPLC chromatogram did not reveal the presence of any free pertechnetate ($^{99m}TcO_4^-$) in the radiolabeled reaction mixture (Fig. 3A). It was further substantiated by TLC analysis in methyl ethyl ketone where no radioactivity was observed at R_f = 1. However, while using water/acetonitrile (1 : 1) as the eluting solvent, considerable radioactivity was observed at R_f = 0, indicating the presence of ^{99m}Tc-colloid. Passing the radiolabeled solution through the C_{18} cartridge could not completely remove colloidal impurities, whereas filtration (0.22 μm) ensured a colloid-free product leading to >99% radiochemical purity and 15 ± 5 GBq μmol^{-1} specific activity. The purification step was essentially carried out before performing any *in vitro* and/or *in vivo* studies.

The lipophilicity of ^{99m}Tc-PSMA-11 was determined by measuring the partition coefficient between octanol and water and the value of $\log P_{o/w}$ was −2.1 ± 0.1. The filtered and purified ^{99m}Tc-PSMA-11 was observed to be stable *in vitro* for 24 h in saline as well in human serum (Fig. 3B). The sufficiently long stability of ^{99m}Tc-PSMA-11 indicates its suitability for performing *in vivo* studies.

In vitro and *in vivo* studies

The radiotracer ^{99m}Tc-PSMA-11 exhibited an uptake of 15.2 ± 1.2% in PSMA-positive prostate carcinoma LNCaP cells, whereas an uptake of 3.8 ± 0.8% was observed in PSMA-negative PC3 cells. The significantly high uptake ($p < 0.005$) in PSMA-positive LNCaP cells and also the significant reduction ($p < 0.005$) in uptake during blocking studies (3.0 ± 0.3%) indicate the receptor specificity of ^{99m}Tc-PSMA-11 (Fig. 4). The cellular uptake was less than that reported for ^{68}Ga-PSMA-11 (23.2 ± 2.2%),[35] but higher than that for ^{99m}Tc-HYNIC-iPSMA (4.5%)[30] and $^{99m}Tc(CO)_3$-labeled PSMA ligand[25] (~10%). Biodistribution studies in normal Swiss mice indicated rapid clearance from blood, liver, intestine, lungs and other major organs (Table 2). The kidney, being a PSMA-expressing and excretory organ, exhibited high uptake at 3 h p.i.

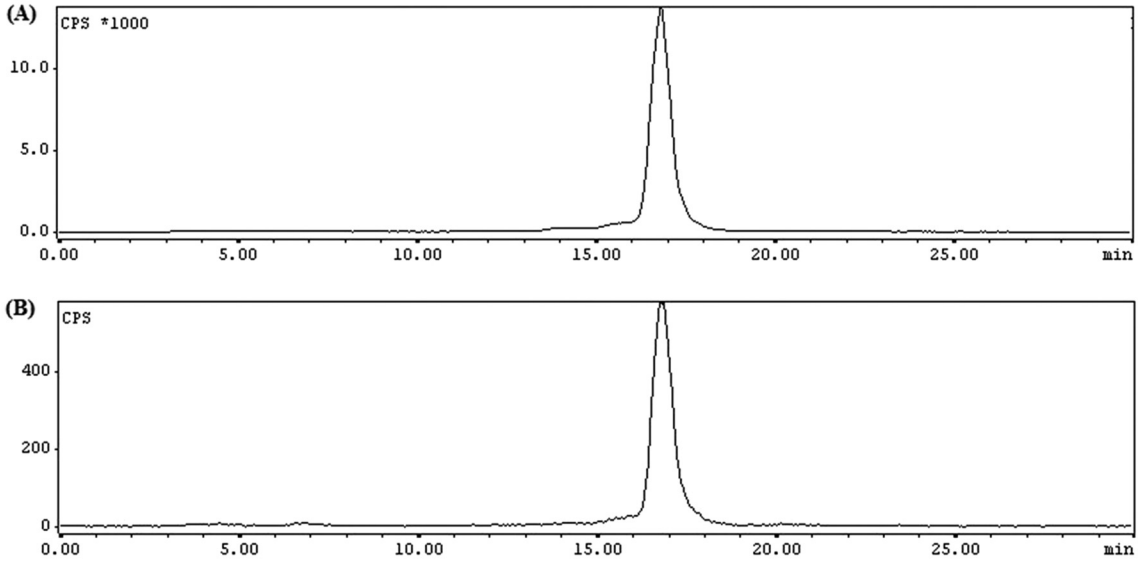

Fig. 3 RP-HPLC radiochromatogram of ^{99m}Tc-PSMA-11: (A) immediately after preparation and (B) after 24 h of incubation in human serum.

Clinical results

SPECT/CT images were acquired by administration of ^{99m}Tc-PSMA-11 in two patients. The first patient aged 50 years with suspected prostate carcinoma on clinical examination and a raised serum prostate specific antigen (PSA) level (7.7 ng mL^{-1}) showed no abnormal tracer uptake in the prostate bed on SPECT–CT and elsewhere in the body during the whole body study (Fig. 5A). Histopathology from the prostate confirmed no malignancy. Intense physiological tracer uptake was noted in the parotid and submandibular salivary glands, kidneys and liver. Other sites of physiological uptake were the spleen, bowel, lacrimal glands, nasal mucosa, and mediastinal blood pool. Another 73 years old male patient with grade III hard nodular prostate on digital rectal examination and raised serum PSA (100 ng mL^{-1}) underwent the ^{99m}Tc-PSMA-11 scan. The patient showed intense uptake in the prostate bed, multifocal uptake in the abdomen, pelvis and left supraclavicular region (Fig. 5B). ^{99m}Tc-PSMA-11 could clearly identify metastasis to retroperitoneal lymph nodes. The histopathology from the core biopsy of the prostate gland confirmed acinar type adenocarcinoma.

Nuclear medicine molecular imaging plays a vital role in cancer care through early and accurate diagnosis. Concerted research efforts have resulted in several PET agents for cancer imaging. However, low resource regions and geographically remote hospitals may not have the medical infrastructure to install expensive imaging equipment or accessibility to a cyclotron. Challenges faced by budget constrained healthcare facilities in rural and isolated locations can be solved by availability of low cost SPECT tracers and equipment. Hence the goal of this study was to prepare a Tc-99m based agent for SPECT imaging of prostate cancer.

SPECT tracers based on ^{99m}Tc-oxo, ^{99m}Tc-HYNIC and ^{99m}Tc(CO)$_3$ cores utilizing chelators and/or linkers well-suited

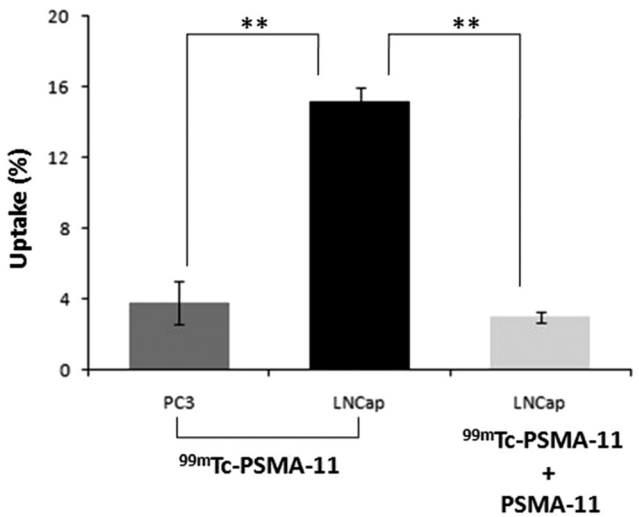

Fig. 4 Uptake of ^{99m}Tc-PSMA-11 in PC3 (PSMA-negative) cells and unblocked and blocked LNCaP cells (PSMA-positive). The error bars represent standard deviation. $^{**}p < 0.005$.

Table 2 Biodistribution studies of ^{99m}Tc-PSMA-11 in normal Swiss mice. Results are expressed as a percentage of the injected dose per gram of tissue (% ID g^{-1}), (mean ± SD, n = 4)

Organs	1 h p.i.	3 h p.i.
Blood	1.2 ± 0.03	0.72 ± 0.04
Liver	1.8 ± 0.1	1.02 ± 0.13
Intestine	2.08 ± 0.23	1.78 ± 0.43
Stomach	2.62 ± 0.2	1.30 ± 0.38
Kidney	42.2 ± 2.9	29.92 ± 3.79
Heart	0.4 ± 0.04	0.34 ± 0.09
Lungs	1.8 ± 0.06	1.03 ± 0.05
Spleen	1.54 ± 0.06	0.84 ± 0.07
Muscle	0.30 ± 0.01	0.20 ± 0.01

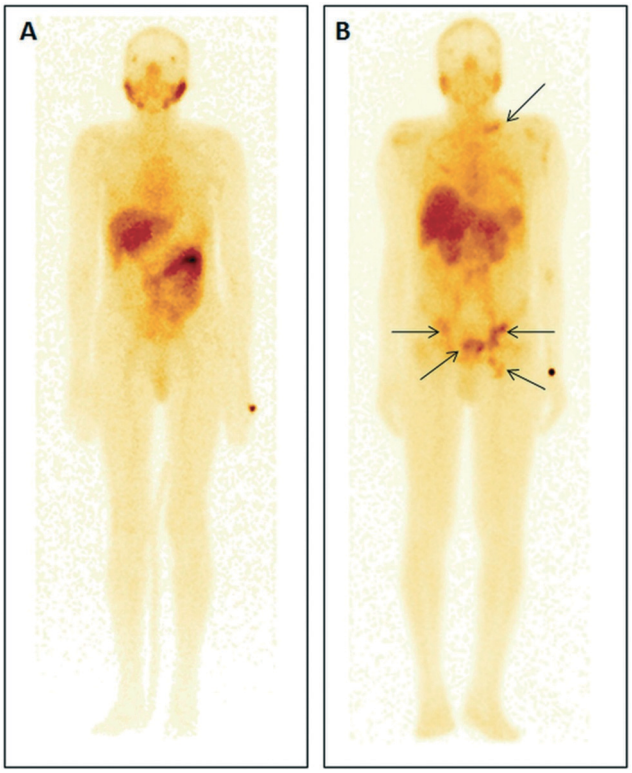

Fig. 5 SPECT/CT images of ^{99m}Tc-PSMA-11 in (A) a 50 year old patient presented with suspected prostate carcinoma but whole body imaging confirmed no uptake in the prostate, only physiological distribution was observed, and (B) a 73 year old patient with confirmed acinar type adenocarcinoma.

for radiolabeling with a particular ^{99m}Tc-core have been developed for prostate cancer imaging. These functionalities regulate the charge, lipophilicity and molecular weight of the metal-chelated ligand and thus affect the pharmacokinetic pattern of the radiotracer. Considering the established potential of ^{68}Ga-PSMA-11 for prostate cancer imaging, we envisioned that Tc-99m labeling of PSMA-11 would not need any alteration in the ligand and therefore exhibit a similar biodistribution pattern. Hence in this study we report the hitherto unexplored possible chelation of Tc-99m with a HBED-CC chelator. Experiments were performed to prove the proposition of the feasibility of ^{99m}Tc-HBED-CC chelate formation. The RP-HPLC radiochromatogram indicated >98% radiolabeling yield of ^{99m}Tc-PSMA-11 with <2% of pertechnetate being present. However 30–35% of radioactivity in the TLC chromatogram was detected to be in the colloidal form. Hence further studies were carried out after filtration (purification) of the radiolabeled product through a 0.22 μm filter leading to >98% radiochemical purity.

Stability studies of ^{99m}Tc-PSMA-11 were conducted in human serum as well in saline. HPLC and TLC chromatograms did not indicate any degradation even after 24 h and hence the radiotracer was considered suitable for performing *in vivo* studies. The radioactivity uptake in the spleen was lower than that of Tc-99m tracers reported by Banerjee *et al.*[27] and Robu *et al.*[29] and comparable to that of ^{99m}Tc-HYNIC-iPSMA reported by Ferro-Flores *et al.*[30] Lung and liver activity was either comparable or less than the reported Tc-99m labeled PSMA targeting tracers. The present radiotracer, ^{99m}Tc-PSMA-11, exhibited favourable pharmacokinetics with rapid clearance from normal tissues. The *in vitro* cellular uptake and *in vivo* biodistribution pattern were conducive to clinical translation of the SPECT tracer. Hence preliminary imaging studies in healthy volunteers and prostate cancer patients were performed.

^{99m}Tc-PSMA-11 exhibited tracer distribution and physiological uptake in concordance to ^{68}Ga-PSMA-11. Preliminary imaging studies indicate that the radiotracer has the potential of visualizing primary and metastatic lesions in patients with good accuracy and specificity and hence studies with ^{99m}Tc-PSMA-11 can be further extended for evaluation in a larger group of patients.

Conclusions

The present study proposes ^{99m}Tc-PSMA-11 as a prospective prostate cancer SPECT imaging agent. The purified ^{99m}Tc-PSMA-11 was tested to be stable in saline as well in human serum. The radiotracer, ^{99m}Tc-PSMA-11, exhibited receptor specificity towards PSMA-positive LNCaP cells and standard physiological distribution in normal mice with rapid clearance from all the major organs at 3 h p.i. Initial studies demonstrate the validity of ^{99m}Tc-PSMA-11 for detection of primary prostate tumor and associated metastatic sites. Detailed investigations would further confirm the diagnostic and treatment monitoring potential of the radiotracer.

Conflicts of interest

The authors declare that there is no conflict of interest in the work reported.

Acknowledgements

The authors are grateful to Dr. P. K. Pujari, Associate Director, Radiochemistry & Isotope Group for his support and encouragement. The help of Radiochemicals Section, Radiopharmaceuticals Division (RPhD), in supplying ^{99}Mo is being thankfully acknowledged. The authors acknowledge the help rendered by the staff of the animal house facility of Bhabha Atomic Research Centre.

References

1 V. Cuccurullo, G. D. Di Stasio and L. Mansi, *World J. Nucl. Med.*, 2018, **17**, 70–78.
2 W. A. Weber and M. J. Morris, *J. Nucl. Med.*, 2016, **57**, 3S–5S.
3 H. Jadvar, *Am. J. Roentgenol. Radium Ther.*, 2012, **19**, 278–291.
4 S. Fanti, S. Minozzi, P. Castellucci, S. Balduzzi, K. Herrmann, B. J. Krause, W. Oyen and A. Chiti, *Eur. J. Nucl. Med. Mol. Imaging*, 2016, **43**, 55–69.

5 A. B. Jani, T. H. Fox, D. Whitaker and D. M. Schuster, *Clin. Nucl. Med.*, 2009, **34**, 279–284.
6 M. H. Umbehr, M. Muntener, T. Hany, T. Sulser and L. M. Bachmann, *Eur. Urol.*, 2013, **64**, 106–117.
7 Y. Chen, M. Pullambhatla, C. A. Foss, Y. Byun, S. Nimmagadda, S. Srinivasan, G. Sgouros, R. C. Mease and M. G. Pomper, *Clin. Cancer Res.*, 2011, **17**, 7645–7653.
8 J. A. Barrett, R. E. Coleman, S. J. Goldsmith, S. Vallabhajosula, N. A. Petry, S. Cho, T. Armor, J. B. Stubbs, K. P. Maresca, M. G. Stabin, J. L. Joyal, W. C. Eckelman and J. W. Babich, *J. Nucl. Med.*, 2013, **54**, 380–387.
9 S. Lütje, S. Heskamp, A. S. Cornelissen, T. D. Poeppel, S. A. M. W. van den Broek, S. Rosenbaum-Krumme, A. Bockisch, M. Gotthardt, M. Rijpkema and O. C. Boerman, *Theranostics*, 2015, **5**, 1388–1401.
10 F. L. Giesel, L. Will, I. Lawal, T. Lengana, C. Kratochwil, M. Vorster, O. Neels, F. Reyneke, U. Haberkon, K. Kopka and M. Sathekge, *J. Nucl. Med.*, 2018, **59**, 1076–1080.
11 F. L. Giesel, K. Knorr, F. Spohn, L. Will, T. Maurer, P. Flechsig, O. Neels, K. Schiller, H. Amaral, W. A. Weber, U. Haberkorn, M. Schwaiger, C. Kratochwil, P. Choyke, V. Kramer, K. Kopka and M. Eiber, *J. Nucl. Med.*, 2018, **60**, 362–368.
12 M. Eiber, T. Maurer, M. Souvatzoglou, A. J. Beer, A. Ruffani, B. Haller, F. P. Graner, H. Kübler, U. Haberkorn, M. Eisenhut, H. J. Wester, J. E. Gschwend and M. Schwaiger, *J. Nucl. Med.*, 2015, **56**, 668–674.
13 J. Müller, D. A. Ferraro, U. J. Muehlematter, H. I. Garcia Schüler, S. Kedzia, D. Eberli, M. Guckenberger, S. G. C. Kroeze, T. Sulser, D. M. Schmid, A. Omlin, A. Müller, T. Zilli, H. John, H. Kranzbuehler, P. A. Kaufmann, G. K. von Schulthess and I. A. Burger, *Eur. J. Nucl. Med. Mol. Imaging*, 2019, **46**, 889–900.
14 A. Farolfi, F. Ceci, P. Castellucci, T. Graziani, G. Siepe, A. Lambertini, R. Schiavina, F. Lodi, A. G. Morganti and S. Fanti, *Eur. J. Nucl. Med. Mol. Imaging*, 2019, **46**, 11–19.
15 U. Bashir, A. Tree, E. Mayer, D. Levine, C. Parker, D. Dearnaley and W. J. G. Oyen, *Eur. J. Nucl. Med. Mol. Imaging*, 2019, **46**, 901–907.
16 I. Rauscher, T. Maurer, W. P. Fendler, W. H. Sommer, M. Schwaiger and M. Eiber, *Cancer Imaging*, 2016, **16**, 14.
17 M. Eiber, G. Weirich, K. Holzapfel, M. Souvatzoglou, B. Haller, I. Rauscher, A. J. Beer, H. J. Wester, J. Gschwend, M. Schwaiger and T. Maurer, *Eur. Urol.*, 2016, **70**, 829–836.
18 I. Rauscher, T. Maurer, A. J. Beer, F. P. Graner, B. Haller, G. Weirich, A. Doherty, J. E. Gschwend, M. Schwaiger and M. Eiber, *J. Nucl. Med.*, 2016, **57**, 1713–1719.
19 M. D. Bartholomä, A. S. Louie, J. F. Valliant and J. Zubieta, *Chem. Rev.*, 2010, **110**, 2903–2920.
20 S. L. Pimlott and A. Sutherland, *Chem. Soc. Rev.*, 2011, **40**, 149–162.
21 I. O. Lawal, A. O. Ankrah, N. P. Mokgoro, M. Vorster, A. Maes and M. M. Sathekge, *Prostate*, 2017, **77**, 1205–1212.
22 M. R. A. Pillai, A. Dash and F. F. Knapp Jr, *J. Nucl. Med.*, 2013, **54**, 313–323.
23 S. S. Jurisson and J. D. Lydon, *Chem. Rev.*, 1999, **99**, 2205–2218.
24 Y. Seo, C. Mari and B. H. Hasegawa, *Semin. Nucl. Med.*, 2008, **38**, 177–198.
25 K. Maresca, J. C. Wang, S. Hillier, F. Femia, G. Lu, C. Zimmerman, J. Kronauge, W. Eckelman, J. Joyal and J. Babich, *J. Nucl. Med.*, 2012, **53**(suppl. 1), 523.
26 S. Vallabhajosula, A. Nikolopoulou, J. W. Babich, J. R. Osborne, S. T. Tagawa, I. Lipai, L. Solnes, K. P. Maresca, T. Armor, J. L. Joyal, R. Crummet, J. B. Stubbs and S. J. Goldsmith, *J. Nucl. Med.*, 2014, **55**, 1791–1798.
27 S. R. Banerjee, M. Pullambhatla, C. A. Foss, A. Falk, Y. Byun, S. Nimmagadda, R. C. Mease and M. G. Pomper, *J. Med. Chem.*, 2013, **56**, 6108–6121.
28 X. Xu, J. Zhang, S. Hu, S. He, X. Bao, G. Ma, J. Luo, J. Cheng and Y. Zhang, *Nucl. Med. Biol.*, 2017, **48**, 69–75.
29 S. Robu, M. Schottelius and M. Eiber, *J. Nucl. Med.*, 2017, **58**, 235–242.
30 G. Ferro-Flores, M. Luna-Gutiérrez, B. Ocampo-García, C. Santos-Cuevas, E. Azorín-Vega, N. Jiménez-Mancilla, E. Orocio-Rodríguez, J. Davanzo and F. O. García-Pérez, *Nucl. Med. Biol.*, 2017, **48**, 36–44.
31 S. Liu, *Adv. Drug Delivery Rev.*, 2008, **60**, 1347–1370.
32 Z. Varasteh, B. Mitran, U. Rosenström, I. Velikyan, M. Rosestedt, G. Lindeberg, J. Sörensen, M. Larhed, V. Tolmachev and A. Orlova, *Nucl. Med. Biol.*, 2015, **42**, 446–454.
33 D. Satpati, R. Sharma, H. D. Sarma and A. Dash, *Chem. Biol. Drug Des.*, 2018, **91**, 781–788.
34 S. Liu and D. S. Edwards, *Chem. Rev.*, 1999, **99**, 2235–2268.
35 M. Eder, M. Schäfer, U. Bauder-Wüst, W. E. Hull, C. Wängler, W. Mier, U. Haberkorn and M. Eisenhut, *Bioconjugate Chem.*, 2012, **23**, 688–697.